ELSEVIER

Nuclear Instruments and Methods in Physics Research B 182 (2001) 174–179

NIM B
Beam Interactions with Materials & Atoms

www.elsevier.com/locate/nimb

Metastable states produced with beam–capillary interaction

Y. Kanai [a,*], K. Ando [a], T. Azuma [d], R. Hutton [a], K. Ishii [e], T. Ikeda [a], Y. Iwai [a,b], K. Komaki [b], K. Kuroki [b], H. Masuda [c], Y. Morishita [a], K. Nishio [c], H. Oyama [a], M. Sekiguchi [f], Y. Yamazaki [a,b]

[a] *Atomic Physics Laboratory, RIKEN, Wako, Saitama 351-0198, Japan*
[b] *Institute of Physics, Graduate School of Arts and Sciences, University of Tokyo, Meguro, Tokyo 153-8902, Japan*
[c] *Department of Industrial Chemistry, Tokyo Metropolitan University, Hachioji, Tokyo 192-0397, Japan*
[d] *Department of Physics, Tokyo Metropolitan University, Hachioji, Tokyo 192-0397, Japan*
[e] *Department of Engineering Science, Kyoto University, Kyoto 606-8501, Japan*
[f] *Center for Nuclear Study, University of Tokyo, Riken Campus, Wako, Saitama 351-0198, Japan*

Abstract

The formation and relaxation processes of hollow atoms and related excited states of ions produced with a Ni microcapillary thin foil have been studied employing various experimental techniques. The first stage of the charge transfer from the surface to the ions was studied by using visible light measurements. On the other hand, X-ray measurements revealed the core electronic configurations of ions at the last moment of the hollow atom evolution. The overall feature of the electron capture processes in the capillary was given by the charge state distribution measurements.

PACS: 34.50.Dy
Keywords: Hollow atoms; Microcapillary; Slow highly charged ions

1. Introduction

When a highly charged ion (HCI) approaches a solid surface, the ion is accelerated toward the surface with its image charge and then the ion resonantly captures target electrons into excited states. According to the classical over barrier (COB) model [1], the distance d_c for the resonant charge transfer to start is given by $\sim(2q)^{1/2}/W$, where q is the charge of the ion and W is the work function of the solid (physical quantities are given in atomic units unless otherwise noted). Such an atom (ion) with multiply excited electrons and inner shell vacancies is called a "hollow atom (ion)". The formation and relaxation dynamics of hollow atoms have been studied intensively in recent years [1–11]. The formation of hollow atoms above the surface was indirectly confirmed through measurements of the angular distribution of reflected ions under glancing angle of incidence [4] or secondary electron yield during

* Corresponding author. Tel.: +81-48-467-9486; fax: +81-48-462-4644.
E-mail address: kanai@rarfaxp.riken.go.jp (Y. Kanai).

0168-583X/01/$ - see front matter
PII: S0168-583X(01)00672-3

neutralization [5]. The deexcitation of hollow atoms proceeds at first via a cascade of autoionization processes. Careful observations of Auger electron spectra in slow HCI–surface collisions indicated that the Auger electrons from hollow atoms above the surface have relatively sharp peak structures, and those below the surface have broader peak structures [6,7]. On the other hand, the emission angular distributions of those two components showed a similar dependence, i.e., cosine-like angular distributions [8], which indicate that both components were rather produced below a surface than above the surface. By using a flat surface target, it is difficult to observe the nature of hollow atom above surface, because its intrinsic lifetime could be longer than the time interval (i.e., $\sim 10^{-13}$ s) between the hollow atom formation above the surface and its arrival at the surface. To overcome the difficulty, hollow atoms (ions) were extracted in vacuum employing a microcapillary target [12–19]. The microcapillary used in our experiments was ~ 1 mm^2 in size with a thickness of $\sim$ μm and had a multitude of a straight holes of ~ 100 nm in diameter. When HCIs impinge on the microcapillary target parallel to the capillary axis, part of the hollow atoms (ions) formed in the capillary can pass through it before hitting the capillary wall. In this case, free hollow atoms are extracted in vacuum. We have used free hollow atoms to study its production and relaxation mechanisms employing the following techniques:

1. visible light measurements, which give information on Rydberg states produced by the first stage of the charge transfer from the capillary surface;
2. X-ray measurements in coincidence with the final charge states, which reveal the lifetime of hollow atoms for different number of electrons transferred;
3. X-ray measurements with a high-resolution grating spectrometer, which allows one to identify the core electronic configurations of hollow atoms;
4. charge state and scattering angle measurements, which are expected to reflect the distance between the ion and the surface at the moment of the charge transfer.

In this paper, we review our research of hollow atoms and related excited states produced by beam–capillary interaction.

2. Visible light measurements

As mentioned in Section 1, when HCIs approach to a solid surface, electrons from the valence band of the solid are resonantly transferred to highly excited state of the ions. According to the COB model, the first electron transfer takes place to

$$n_c \sim q/[2W(1 + (q - 0.5)/(8q)^{1/2})]^{1/2}$$

of the incident ions [20]. By adapting a reasonable value of 0.2 a.u. for W, n_c is estimated to be $q + 1$. Those atoms (ions) may emit visible light via transitions among highly excited states. In order to see what really happens, visible light emitted from the ions transmitted through a Ni capillary were measured with a Czerny–Turner type spectrometer with one-to-one imaging mirrors. Spectra for 2.0 keV/u Ar^{q+} ($6 \leqslant q \leqslant 10$) ions are shown in Fig. 1 [17,21,22]. Several lines are attributed to $\Delta n = 1$ transitions of the ions which have captured an electron into high Rydberg states, the transition wavelengths of which can be well accounted for by assuming energy levels as those of hydrogenic ions. For example, in the case of the Ar^{8+} incident ion, transition wavelengths of Ar^{7+} from $1s^2 2s^2 2p^6 nl$ to $1s^2 2s^2 2p^6 (n-1) l'$ states are calculated to be 298, 434, 607 and 820 nm for $n = 8$, 9, 10 and 11, respectively (k, l, m and n in Fig. 1). Similarly, intense lines referred to as $a, b, \ldots, u$ in Fig. 1 can be attributed to $\Delta n = 1$ transitions from the initial states n, where $q - 1 \leqslant n \leqslant q + 3$, the central value of which is just that predicted by the COB model.

It is noted that the lines observed for Ar^{q+} incident ions can also be observed at the same wavelength, in the present spectral resolution, for $Ar^{(q+1)+}$ ($Ar^{(q+2)+}$) incident ions, which are labeled by primed letters like k' (k'') in Fig. 1. This indicates that $Ar^{(q+1)+}$ ($Ar^{(q+2)+}$) ion has captured many electrons in the capillary, and deexcited through radiative or Auger transitions leaving one electron in its high Rydberg states.

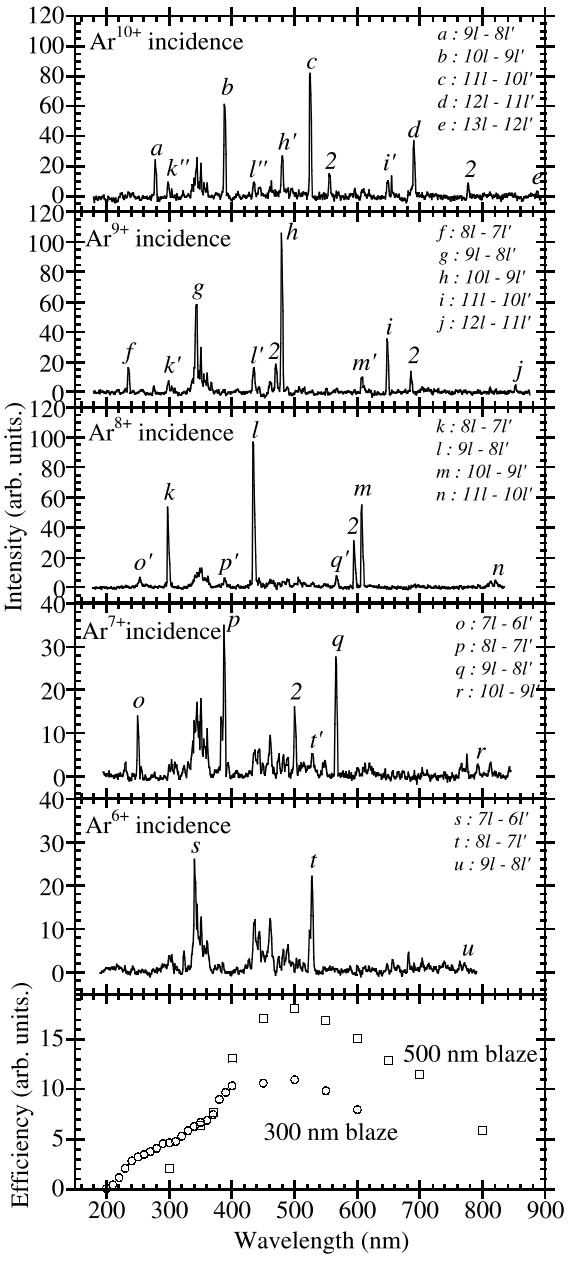

Fig. 1. Visible light spectra observed for Ar^{q+} $(6 \leqslant q \leqslant 10)$ incident ions downstream of the capillary target and relative efficiency curves of the detection system. "2" indicates the 2nd-order reflection of the grating. For details see the text.

3. X-ray measurements in coincidence with final charge states

To measure the X-rays emitted during transitions into inner shell holes in coincidence with the final charge state gives us information on the total number of electrons in outer shells still keeping the inner shell holes.

K X-rays emitted from 2.3 keV/u N^{6+} ions were measured in coincidence with the final charge state q_f of the transmitted ions through a Ni capillary [15]. The lifetime of the K-shell hole of transmitted ions was determined through measurements of integrated delayed X-ray yield, the intensity of which is given by

$$\eta(t_d, q_f) = \eta(z/v, q_f) = \int_{z/v}^{\infty} \zeta(z'/v, q_f)\, d(z'/v), \quad (1)$$

where $\zeta(z'/v, q_f)$ is the differential intensity of X-rays emitted from the ions with their final charge states q_f at z' from the target, v is the projectile velocity, t_d is given by z/v. The integrated delayed X-ray yields $\eta(t_d, q_f)$ normalized per $N^{q_f^+}$ ion with $q_f = 5$, 4, 3 and 2 are shown in Fig. 2. The time resolution was ~1 ns. A considerable fraction of the transferred ions with a K-shell hole were found to be in extremely stabilized states. The yields of the delayed K X-rays for $q_f = 5$, 4, 3 and 2 were ~8%, ~4%, ~1% and ~0.5%, respectively. It can be seen that (1) the X-ray emission from the

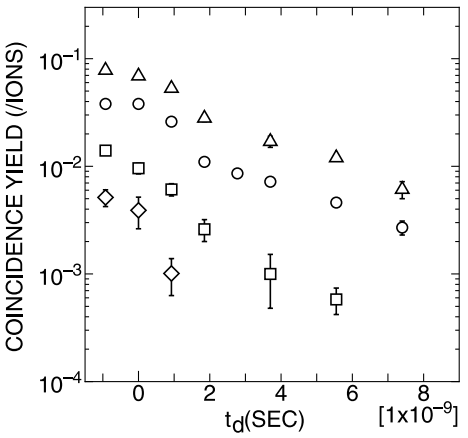

Fig. 2. The integrated delayed X-ray yields normalized per one $Ne^{q_f^+}$ ion; $q_f = 5$ (△), 4 (○), 3 (□) and 2 (◇) [15].

stabilized states was observed not only from a few electron systems but also from multielectron systems, e.g., a 5 electron system ($q_f = 2$), and (2) the decay curves of the N K-shell hole depended only weakly on the final charge state, and consisted of at least two components for $q_f = 5$, 4 and 3. The lifetimes of the longer components were ~4, ~4 and ~2.5 ns for $q_f = 5$, 4 and 3, respectively, which are several orders of magnitude longer than typical lifetimes of a N K-hole with filled L shell.

The peak energy of X-rays was ~420 eV, which is ~30 eV higher than that observed for a flat Al target [15], i.e., the number of L-shell electrons is very small. This feature did not depend on the q_f and delay time after the capillary target. This indicates that the core configurations of the excited states for longer lifetimes are in spin-aligned metastable states [15].

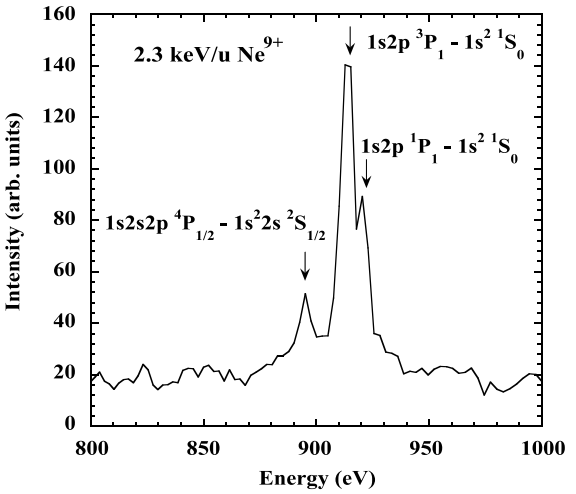

Fig. 3. Spectra of K X-rays measured with the spectrometer, for 2.3 keV/u Ne^{9+} ions transmitted through a Ni capillary target. Core configurations of excited states are indicated.

4. High-resolution X-ray measurements

The energy resolution of Si(Li) detector is not enough to identify the electronic configurations involved in the X-ray emission, which is very important to understand the dynamics of the hollow atom formation and relaxation processes. In order to overcome the difficulty, we developed a high-resolution soft X-ray spectrometer, which consists of a grating with varied groove spacing and a back-illuminated charged couples device (CCD) [23]. The energy resolution of the spectrometer was ~2.6 eV full width at half maximum at ~900 eV. The K X-ray spectra taken with the spectrometer for 2.3 keV/u Ne^{9+} ions transmitted through the Ni capillary are shown in Fig. 3. Three sharp peaks are seen at 921.7, 913.4 and 895.4 eV. Comparison with theoretical calculation [24] and reference data [14] indicates that the core electronic states of these peaks can be attributed to He-like 1s2p ^{1}P–1s^2 ^{1}S (922.1 eV), 1s2p ^{3}P–1s^2 ^{1}S (914.9 eV) and Li-like 1s2s2p ^{4}P–1s^{2}2s ^{2}S (895.0 eV), respectively. The observed energies and the reference data for the transitions with their core configurations are summarized in Table 1. The decay curve of X-rays emitted from 9 keV/u Ne^{9+} ions with an Si(Li) detector showed that the lifetime of the upper state is ~0.8 ns, which indicated that the state involved was 1s2s2p ^{4}P states because the predicted lifetimes of 1s2s2p $^4P_{1/2}$, $^4P_{3/2}$ and $^4P_{5/2}$ are 0.4, 0.6 and 12 ns [14,16]. The $^4P_{5/2}$ state decays only through the Auger transition, and do not contribute to X-ray spectra [14,16]. This assignment is re-confirmed with the high-resolution measurements, which reveled that the transition energy is just as is predicted.

The observed transition energies are in good agreement with reference data as shown in Table 1.

Table 1
Electronic core configuration of Ne ions after the Ni capillary

Experiment	Ref. data	Core configuration	Terms
913.4 ± 1.3 eV	914.9 eV [24]	1s2p → 1s^2	$^3P_1$–$^1S_0$
921.7 ± 1.3 eV	922.1 eV [24]	1s2p → 1s^2	$^1P_1$–$^1S_0$
895.4 ± 1.3 eV	895.0 eV [14]	1s2s2p → 1s^{2}2s	$^4P_{1/2,3/2}$–$^1S_0$

From our measurements, we have not obtained the direct evidence for the existence of spectator electrons in Rydberg states at the moment of K X-ray emissions. High-resolution X-ray measurements in coincidence with the final charge state will reveal this point. However, the efficiency of the grating X-ray spectrometer is too small to do the coincidence measurements. We have just started to introduce a superconducting tunnel junction (STJ) X-ray detector [25,26] to make coincidence experiments possible still keeping the energy resolution quite high. The energy resolution of an STJ detector is typically ~5 eV at 900 eV with high efficiency ~90%. Up to now, we have measured X-rays emitted from slow HCIs bombarding a flat surface, and obtained ~30 eV energy resolution at 900 eV with the STJ detector [27].

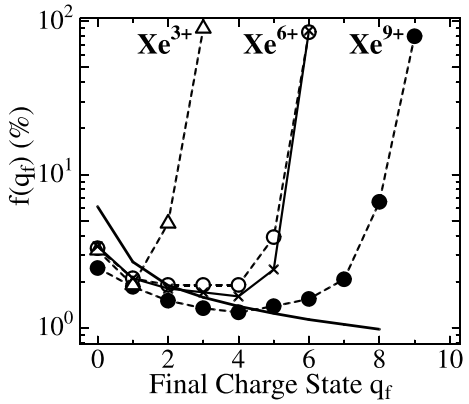

Fig. 4. Final charge state distributions for 900 eV/q Xe^{q+} ($q = 3$, 6, 9) ions after the capillary target. Experimental results for Xe^{3+} (△), Xe^{6+} (○) and Xe^{9+} (●). Calculated results without Auger deexcitation (—) and with Auger deexcitation (×).

5. Charge state distributions

Charge state distributions of Xe ions, which deexcited into ground state, were measured. Typical final charge state distributions for 800 eV/q Xe^{q+}, $q = 3$, 6, 9 are shown in Fig. 4, which are all "U-shaped" for all the incident charge states measured. The final charge state distribution can be roughly estimated with d_c, which is shown by the solid line for $q = 6$ in Fig. 4. It is seen that the general behavior for low q_f region is more or less reproduced, but it deviates from the observation for high q_f region, which may be explained with Auger processes. A Monte Carlo simulation taking into account Auger processes has been made for Xe^{6+} ion by Tökési et al. [28,29], the results of which is shown by the solid line in Fig. 4. It is seen that the agreement with our measurements for the Xe^{6+} incident case is quite satisfactory.

The angular distributions for each exiting ions are shown in Fig. 5. It is seen that ions with higher q_f are more deflected than those with lower q_f, which is not consistent with a qualitative expectation. Actually, the angular distribution of 2.1 keV/u N^{6+} transmitted through a Ni capillary calculated by Tökési et al. [28] showed same features as the qualitative expectation, which do not agree with the experiments. In order to study this puzzling but interesting discrepancies, a new

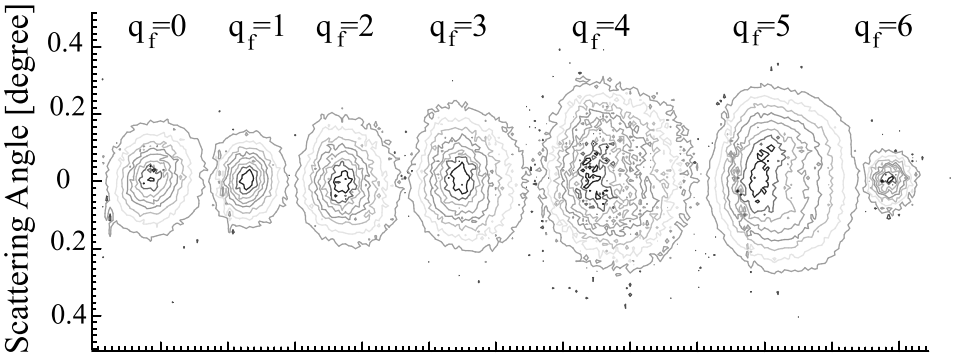

Fig. 5. 2-dimensional contour plots of $Xe^{q_f^+}$ for Xe^{6+} incident. Each contour is normalized at its peak height.

measurement employing other targets with much straight capillary are under preparation.

6. Summary

With various experimental techniques, the nature and the relaxation processes of hollow atoms or related excited ions produced by the thin capillary target have become clear. Visible light measurements gave the evidence that multielectrons transfer into ions from the capillary and those ions are stabilized with one electron in the Rydberg state. From X-ray measurements in coincidence with the final charge state, the production of spin-aligned states in the capillaries was discussed. High-resolution X-ray measurements reveal core electronic configurations of ions after the capillary at the moment of the X-ray emission. Charge state distributions of ions passing through the capillary are qualitatively in agreement with the Monte Carlo simulation [28,29], which means that the simulation can reproduce crude features of the ion capillary interactions.

References

[1] J. Burgdörfer, P. Lerner, F.W. Meyer, Phys. Rev. A 44 (1991) 5674.
[2] J.P. Briand, L. de Billy, P. Charles, S. Essabaa, Phys. Rev. Lett. 65 (1990) 159.
[3] H.J. Andrá, A. Simionovici, T. Lamy, A. Brenac, G. Lamboley, J.J. Bonnet, A. Fleury, M. Bonnefoy, M. Chassevent, S. Andriamonje, A. Pesnell, Z. Phys. D 21 (1991) S135.
[4] H. Winter, Europhys. Lett. 18 (1992) 207.
[5] F. Aumayr, H. Kurz, D. Shneider, M. Briere, J.W. McDonald, C.E. Cunningham, HP. Winter, Phys. Rev. Lett. 71 (1993) 1943.
[6] F.W. Meyer, S.H. Overbury, C.C. Havener, P.A. Zeijmans van Emmichoven, D.M. Zehner, Phys. Rev. Lett. 67 (1991) 723.
[7] J. Das, R. Morgenstern, Phys. Rev. A. 47 (1993) R755.
[8] R. Köhrbrück, M. Grether, A. Spieler, N. Stolterfoht, Phys. Rev. A 50 (1994) 1429.
[9] L. Folkerts, S. Schippers, D.M. Zehner, F.W. Meyer, Phys. Rev. Lett. 74 (1995) 2204.
[10] K. Kakutani, T. Azuma, Y. Yamazaki, K. Komaki, K. Kuroda, Jpn J. Appl. Phys. 34 (1995) L580.
[11] T. Neidhart, F. Pichler, F. Aumayr, HP. Winter, M. Schmid, P. Varga, Phys. Rev. Lett. 74 (1995) 5280.
[12] H. Masuda, K. Fukuda, Science 268 (1995) 1466.
[13] H. Masuda, M. Satoh, Jpn. J. Appl. Phys. 35 (1996) L126.
[14] Y. Yamazaki, S. Ninomiya, F. Koike, H. Masuda, T. Azuma, K. Komaki, K. Kuroki, M. Sekiguchi, J. Phys. Soc. Jpn. 65 (1996) 1199.
[15] S. Ninomiya, Y. Yamazaki, F. Koike, H. Masuda, T. Azuma, K. Komaki, K. Kuroki, M. Sekiguchi, Phys. Rev. Lett. 78 (1997) 4557.
[16] S. Ninomiya, Y. Yamazaki, T. Azuma, K. Komaki, F. Koike, H. Masuda, K. Kuroki, M. Sekiguchi, Phys. Scr. T 73 (1997) 316.
[17] Y. Morishita, S. Ninomiya, Y. Yamazaki, K. Komaki, K. Kuroki, H. Masuda, M. Sekiguchi, Phys. Scr. T 80 (1999) 212.
[18] Y. Yamazaki, Phys. Scr. T 73 (1997) 293.
[19] Y. Yamazaki, Int. J. Mass Spectrom. 192 (1999) 437.
[20] J. Burgdörfer, in: C.D. Lin (Ed.), Review of Fundamental Processes and Applications of Atoms and Ions, World Scientific, Singapore, 1993, p. 517.
[21] H.A. Torii, Y. Morishita, Y. Yamazaki, K. Komaki, K. Kuroki, R. Hutton, K. Ishii, K. Ando, H. Masuda, M. Sekiguchi, M. Hori, E. Widmann, R.S. Hayano, RIKEN Rev. 31 (2000) 30.
[22] Y. Morishita, H.A. Torii, Y. Yamazaki, K. Komaki, K. Kuroki, R. Hutton, A. Ando, K. Ishii, H. Masuda, M. Sekiguchi, To be published.
[23] Y. Iwai, S. Thuriez, Y. Kanai, H. Oyama, K. Ando, R. Hutton, H. Masuda, K. Nishio, K. Komaki, Y. Yamazaki, RIKEN Rev. 31 (2000) 34.
[24] R.L. Kelly, J. Phys. Chem. Ref. Data 16 (Suppl. 1) (1987).
[25] H. Sato, Y. Takizawa, W. Ootani, T. Ikeda, T. Oku, C. Otani, H. Watanabe, K. Kawai, H. Miyasawa, H. Kato, H.M. Shimizu, H. Nakagawa, H. Akoh, M. Aoyagi, T. Taino, Jpn. J. Appl. Phys. 39 (2000) 5090.
[26] H.M. Shimizu, T. Ikeda, H. Kato, K. Kawai, H. Miyasaka, T. Oku, W. Ootani, C. Otani, H. Sato, Y. Takizawa, H. Watanabe, RIKEN Rev. 31 (2000) 74.
[27] T. Ikeda, H. Kato, H. Sato, K. Kawai, H. Miyasaka, T. Oku, C. Otani, H.M. Shimizu, Y. Takizawa, H. Watanabe, H. Nakagawa, H. Akoh, M. Aoyagi, T. Taino, IEEE Trans. Appl. Superconductivity, To be published.
[28] K. Tökési, L. Wirtz, C. Lemell, J. Burgdörfer, Phys. Rev. A 61 (2000) 020901(R).
[29] K. Tökési, Private communications.